

# Flow development in the vicinity of the sharp trailing edge on bodies impulsively set into motion

By JAMES C. WILLIAMS

Department of Aerospace Engineering, Auburn University, Auburn, Alabama

(Received 30 March 1981)

The initial development of the viscous flow in the vicinity of the sharp trailing edge of a symmetrical body, impulsively set into motion is studied within the framework of boundary-layer theory. For a blunt trailing edge there exists a similarity solution for the inviscid outer flow as has been pointed out by Proudman & Johnson (1961). The present work shows that for sharp trailing edges, however, no such solution exists.

For small or moderate trailing-edge angles, a moving singularity occurs in the solution fairly early in the flow development. The flow in the vicinity of this singularity exhibits the characteristics of unsteady separation. For large trailing-edge angles, the boundary layer becomes so thick that solutions must be terminated before there is any evidence of a singularity. For a cusped trailing edge, the solution is arbitrarily terminated to avoid large computational times and with the realization that the trailing edge flow must eventually be influenced by the leading edge at which time the present solutions cease to have meaning.

---

## 1. Introduction

When a symmetrical body is impulsively set into motion, at time  $t = 0$ , with a uniform motion along the plane of symmetry, the inviscid flow over the body develops instantaneously. This flow is the classical irrotational flow. On the other hand, the flow within the viscous layer adjacent to the body develops slowly, reaching a fully developed unsteady flow only after some period of time.

The development of this viscous layer actually occurs in two stages. For small times, the viscous flow is dominated by local forces and accelerations; the local flow is independent of conditions far upstream and in particular at the leading edge of the body. At some later time the influence of the leading edge comes into play and the flow develops under the influence of both local conditions and the conditions far upstream (at the leading edge). This dual development of the viscous layer has been demonstrated in the case of a flat plate by Stewartson (1951), Hall (1969) and Dennis (1972) and in the case of wedges by Smith (1967), Nanbu (1971) and Williams & Rhyne (1980).

In the present brief note we investigate the first phase of the unsteady development, according to the boundary-layer equations, of the viscous flow in the vicinity of a rear stagnation point on a body with a sharp trailing edge. An appropriate idealization for such a flow appears to be the flow in the vicinity of a wedge with the flow leaving the wedge (as opposed to flowing onto the wedge). For this flow a potential flow solution is known. This potential flow solution is taken as the instantaneously developed inviscid

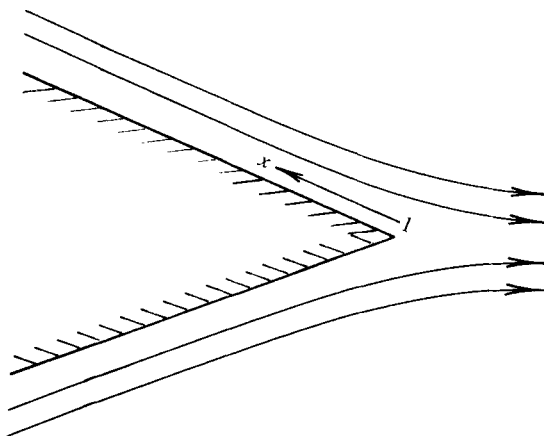


FIGURE 1. Flow geometry for flow near a rear stagnation point.

flow in the vicinity of the sharp trailing edge and the initial development of the viscous layer, resulting from this potential flow is investigated.

Such an analysis may be considered as a logical extension of the work of Proudman & Johnson (1961) who investigated the unsteady development according to the Navier–Stokes equations, of the viscous flow in the vicinity of a rear stagnation point on a bluff body impulsively set into motion. Indeed, one member of the family of flows investigated herein is exactly the flow studied by Proudman & Johnson and later re-examined by Robins & Howarth (1972). It is shown that only in the case of a bluff body (a trailing-edge-included angle of  $180^\circ$ ) does there exist a large-time similarity solution for the outer inviscid flow which scales exponentially with time. The results of this investigation indicate that for small or moderately sharp trailing edges a moving singularity occurs quite early in the flow development. Furthermore, the flow in the vicinity of this moving singularity has just the characteristics postulated in the Moore–Rott–Sears model for unsteady boundary-layer separation. For large trailing-edge angles, the boundary layer appears to become excessively thick and no indication of a separation singularity is found prior to the termination of the solution on the basis of the boundary-layer thickness.

## 2. Analysis

We consider the inviscid (irrotational) flow field in the vicinity of a sharp trailing edge on a symmetrical body which has been impulsively set into motion at time  $t = 0$ . The flow in the neighbourhood of the sharp trailing edge is idealized by considering the flow *off* a wedge (figure 1). Let  $x$  and  $y$  be co-ordinates measured, respectively, along the surface from the trailing edge and normal to the surface of the body. The corresponding velocity components are  $u$  and  $v$ , respectively. The potential flow solution for the idealized flow in the neighbourhood of the trailing edge is simply the inverse of the potential flow for a sharp wedge. The stream function in this case is given by

$$\psi = \frac{Cr^{m+1}}{(m+1)} \sin [(m+1)\theta], \quad (1)$$

where  $r$  and  $\theta$  are conventional polar co-ordinates, and the velocity component parallel to the surface, denoted by  $u_\delta$  is simply

$$u_\delta = -cx^m. \quad (2)$$

Here  $m$  is related to the internal angle of the trailing edge,  $\beta\pi$ , by

$$\beta\pi = 2\pi m/(m+1).$$

This is the inviscid flow which develops instantaneously when the body is impulsively set into motion. We now turn our attention to the initial development of the viscous boundary layer, bounded on one side by the body and on the other by the foregoing inviscid flow. The unsteady development of this boundary layer is described by the usual boundary-layer equations:

$$\frac{\partial u}{\partial x} + \frac{\partial v}{\partial y} = 0, \quad \frac{\partial u}{\partial t} + u \frac{\partial u}{\partial x} + v \frac{\partial u}{\partial y} = \frac{\partial u_\delta}{\partial t} + u_\delta \frac{\partial u_\delta}{\partial x} + \nu \frac{\partial^2 u}{\partial y^2}, \quad (4)$$

where  $t$  is time and  $\nu$  is the kinematic viscosity of the fluid. The appropriate boundary conditions for this problem are the no-slip and impermeable wall conditions at the wall:

$$u(x, 0, t) = v(x, 0, t) = 0 \quad (5)$$

and the condition that the viscous flow passes over to inviscid flow at large  $y$ :

$$\lim_{y \rightarrow \infty} u(x, y, t) = u_\delta(x, t) = -cx^m. \quad (6)$$

The problem at hand is to determine the development of the velocity field  $(u, v)$  as a function of the spatial co-ordinates  $x$  and  $y$ , and of time  $t$ . Clearly the problem is one of three independent variables  $(x, y, t)$ . The number of independent variables may be reduced to two by an appropriate scaling. An appropriate scaling for the present problem may be found either by the formal technique of semi-similar solutions (Williams & Johnson 1974) or on the basis of dimensional considerations. In either case, it is possible to show that two new scaled co-ordinates are

$$\eta = y \left( \frac{G_1(\xi) cx^{m-1}}{\nu} \right)^{\frac{1}{2}}, \quad \xi = G_2(-cx^{m-1}t),$$

where  $G_1(\xi)$  and  $G_2(-cx^{m-1}t)$  are two arbitrary functions. Consider first the case where these functions are chosen so that

$$G_1(\xi) = \frac{1-\xi}{\xi}, \quad G_2 = 1 - \exp[-2cx^{m-1}t].$$

That is

$$\eta = y \left( \frac{(1-\xi) cx^{m-1}}{\nu \xi} \right)^{\frac{1}{2}}, \quad \xi = 1 - \exp[-2cx^{m-1}t]. \quad (7)$$

This choice of the functions  $G_1$  and  $G_2$  is made for a very practical reason. Note that this particular choice for the functional form of  $\xi$  collapses the infinite interval of integration,  $0 \leq t \leq \infty$ , into a finite interval  $0 \leq \xi \leq 1$ . The choice of the functional form of  $G_1$  in the  $y$  scaling is made so that for small time  $\eta \simeq y/t^{\frac{1}{2}}$ , which is the appropriate scaling for small-time problems (this is the so-called Rayleigh scaling) while for large time  $\eta \simeq y/e^t$ . This latter scaling is the one suggested by Proudman &

Johnson (1961) for the large-time solution to the bluff-body rear-stagnation-point problem.

The above scalings are used together with a dimensionless stream function  $f(\xi, \eta)$  defined by

$$\psi(c, y, t) = - \left( \frac{vcx^{m+1}\xi}{(1-\xi)} \right)^{\frac{1}{2}} f(\xi, \eta). \quad (8)$$

The continuity equation is satisfied identically and the momentum equation becomes:

$$\begin{aligned} \frac{\partial^3 f}{\partial \eta^3} - \left\{ \frac{m\xi}{(1-\xi)} + \frac{(1-m)}{2(1-\xi)} \left[ \xi + \ln(1-\xi) \right] \right\} f \frac{\partial^2 f}{\partial \eta^2} \\ - \frac{m\xi}{(1-\xi)} \left\{ 1 - \left( \frac{\partial f}{\partial \eta} \right)^2 \right\} + \frac{\eta}{(1-\xi)} \frac{\partial^2 f}{\partial \eta^2} - 2\xi \frac{\partial^2 f}{\partial \xi \partial \eta} \\ - (1-m)\xi \ln(1-\xi) \left\{ \frac{\partial^2 f}{\partial \eta^2} \frac{\partial f}{\partial \xi} - \frac{\partial f}{\partial \eta} \frac{\partial^2 f}{\partial \eta \partial \xi} \right\} = 0. \end{aligned} \quad (9)$$

The appropriate boundary conditions for this problem, in the transformed co-ordinates, are

$$f(\xi, 0) = \frac{\partial f}{\partial \eta}(\xi, 0) = 0, \quad \lim_{\eta \rightarrow \infty} \frac{\partial f}{\partial \eta}(\xi, \eta) = 1. \quad (10), (11)$$

We note that in the case where  $m = 1$ , equation (9) becomes

$$\frac{\partial^3 f}{\partial \eta^3} - \frac{\xi}{(1-\xi)} f \frac{\partial^2 f}{\partial \eta^2} - \frac{\xi}{(1-\xi)} \left\{ 1 - \left( \frac{\partial f}{\partial \eta} \right)^2 \right\} + \frac{\eta}{(1-\xi)} \frac{\partial^2 f}{\partial \eta^2} - 2\xi \frac{\partial^2 f}{\partial \xi \partial \eta} = 0. \quad (12)$$

Now if we ignore the viscous term and take the limit as  $\xi \rightarrow 1$ , equation (12) reduces to

$$(f - \eta) \frac{\partial^2 f}{\partial \eta^2} + 1 - \left( \frac{\partial f}{\partial \eta} \right)^2 = 0. \quad (13)$$

This is the equation whose solution describes the outer inviscid flow at large times (equation (14) of Proudman & Johnson 1961; equation (3.1) of Robins & Howarth 1972). A close inspection of equation (9) indicates that such a similarity equation does not exist if  $m \neq 1$ ; i.e. there is no similarity solution to the outer inviscid flow field at large times ( $\xi \rightarrow 1$ ).

The scalings given by equations (7), while appropriate in demonstrating the existence or non-existence of a similar solution for the inviscid portion of the flow at large times, are not appropriate for numerical computation of the flow field. We seek other scalings for this purpose. In this quest, we are guided by the fact, noted by Proudman & Johnson, that for large times the flow near the wall at the rear stagnation point approaches a steady flow *towards* the stagnation point and therefore the skin-friction coefficient tends to a finite negative value, equal in magnitude to the skin friction at a front stagnation point. This fact suggests that the appropriate scaling for flows in the vicinity of the sharp trailing edge, at large time may simply be the Falkner-Skan scaling. For small time, however, the appropriate scaling is still the Rayleigh scaling which is independent of  $x$ . To obtain the desired scaling which has the proper small-time and large-time behaviour, we introduce

$$G_1 = 1/\xi \quad \text{and} \quad G_2 = 1 - \exp[-cx^{m-1}t] \quad (14)$$

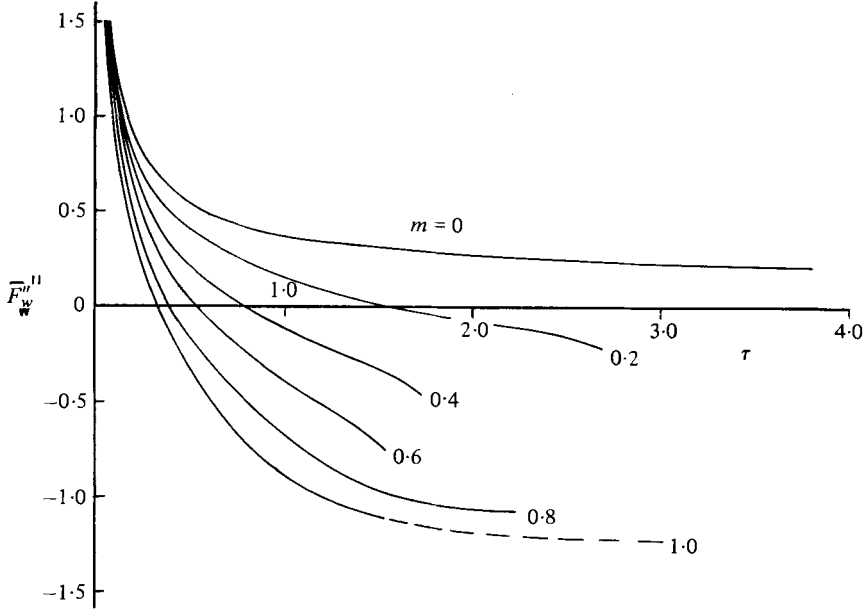


FIGURE 2. Variation of the normalized wall shear with the non-dimensional time,  $\tau$ , for various values of  $m$ .

so that

$$\eta = y \left( \frac{cx^{m-1}}{\nu\xi} \right), \quad \xi = 1 - \exp[-cx^{m-1}t]. \quad (15)$$

Clearly  $\eta$  behaves as  $y/t^{\frac{1}{2}}$  for small time and as  $y(cx^m/x)^{\frac{1}{2}}$  for large time, the desired behaviour for these scalings. With a non-dimensional stream function defined by  $\psi = -(\nu cx^{m+1}\xi)^{\frac{1}{2}} f(\xi, \eta)$ , the reduced momentum equation becomes

$$\begin{aligned} \frac{\partial^2 f}{\partial \eta^3} - \{m\xi + (1-m)[\xi + (1-\xi)\ln(1-\xi)]/2\} f \frac{\partial^2 f}{\partial \eta^2} \\ - m\xi \left\{ 1 - \left( \frac{\partial f}{\partial \eta} \right)^2 \right\} + -\xi(1-\xi) \frac{\partial^2 f}{\partial \xi \partial \eta} + \frac{1}{2}(1-\xi) \eta \frac{\partial^2 f}{\partial \eta^2} \\ + (m-1)(1-\xi) \ln(1-\xi) \left\{ \frac{\partial f}{\partial \xi} \frac{\partial^2 f}{\partial \eta^2} - \frac{\partial f}{\partial \eta} \frac{\partial^2 f}{\partial \xi \partial \eta} \right\} = 0. \end{aligned} \quad (16)$$

For simplicity in computing, equation (16) as written as a pair of equations:

$$\frac{\partial^2 w}{\partial \eta^2} + \alpha_1 \frac{\partial w}{\partial \eta} + \alpha_2 w + \alpha_3 = \alpha_4 \frac{\partial w}{\partial \xi}, \quad \frac{\partial f}{\partial \eta} = w, \quad (17a, b)$$

in which

$$\alpha_1 = -\{m\xi + \frac{1}{2}(1-m)[\xi + (1-\xi)\ln(1-\xi)]\} f + \frac{1}{2}(1-\xi)\eta + (m-1)(1-\xi)\ln(1-\xi) \partial f / \partial \xi, \\ \alpha_2 = m\xi \partial f / \partial \eta, \quad \alpha_3 = -m\xi, \quad \alpha_4 = (1-\xi) \{ \xi + (m-1) \ln(1-\xi) \} \partial f / \partial \eta.$$

In this new system of two equations, the boundary conditions become:

$$w(\xi, 0) = f(\xi, 0) = 0, \quad \lim_{\eta \rightarrow \infty} w(\xi, \eta) = 1. \quad (18)$$

Equations (17a, b), subject to the boundary conditions given by (18), have been

solved using an implicit finite-difference scheme, similar to that proposed by Blottner (1972). Results have been obtained for values of  $m$  of 0, 0.2, 0.4, 0.6, 0.8, and 1.0 corresponding to, within the limits of this model, trailing-edge-included angles of 0, 1.047, 1.795, 2.356 and  $\pi$  radians, respectively.

The solution of equation (16) (or alternately of (17*a*, *b*)) is started at  $\xi = 0$  where equation (16) becomes

$$\frac{\partial^3 f}{\partial \eta^3} + \frac{\eta}{2} \frac{\partial^2 f}{\partial \eta^2} = 0.$$

The solution to this equation is straightforward and extremely simple. It is, in fact, the classical Rayleigh solution for the flow past an infinite flat plate, impulsively set into motion. Once the solution at  $\xi = 0$  is known, solutions at subsequent stations are obtained by a straight-forward marching technique.

### 3. Results

Results for the normalized skin-friction coefficient

$$F_w'' = (vx/(cx^m)^3)^{\frac{1}{2}} \left. \frac{\partial u}{\partial y} \right|_{y=0} = f''(\xi, 0)/\xi^{\frac{1}{2}}$$

are presented in figure 2 as a function of the normalized time  $\tau$  defined by  $\frac{1}{2}cx^{m-1}t$ . Here results are presented for values of  $m$  of 0, 0.2, 0.4, 0.6, 0.8 and 1.0.

The calculations which lead to these results were terminated one of three ways, depending upon the manner in which the solution proceeds. For  $m = 0$  (the trailing edge of a flat plate) the normalized skin friction appeared to approach zero as  $\tau$  becomes large. For this case, the solution was arbitrarily terminated at a value of  $\tau$  of approximately 3.8 to avoid excessive computer time. Furthermore, the present analysis is only valid for a limited time. As pointed out earlier, the development of the boundary layer, after an impulsive start, occurs in two phases. The first of these, which is being calculated here, is independent of the conditions upstream, particularly at the leading edge of the body. This phase is terminated when the presence of the leading edge is felt at the station in question. The time required for the effect of the leading edge to be transmitted to a given local station is proportional to the distance between the leading edge and the local station and inversely proportional to the average speed, at the upper edge of the boundary layer, between the leading edge and the point in question. Obviously, the time required for the effect of the leading edge to be 'felt' locally can be altered by changing the shape of the body upstream from the point in question. However, the influence of the leading edge, at the trailing edge, cannot be delayed indefinitely. It was therefore felt that it was not realistic to extend the calculations indefinitely since sooner or later the effects of the leading edge would be felt.

For  $m = 0.8$  and  $m = 1.0$  the computations were terminated at moderate values of  $\tau$  because the boundary-layer thickness exceeded an arbitrary value corresponding to  $\eta = 60$ . The validity of the calculations for  $m = 0.8$  when the boundary layer becomes excessively thick is certainly open to question. On the other hand, the solution for  $m = 1.0$  is a solution to the full Navier-Stokes equations and therefore is not limited by the boundary layer assumptions. The extension of the solution for  $m = 1.0$ , beyond

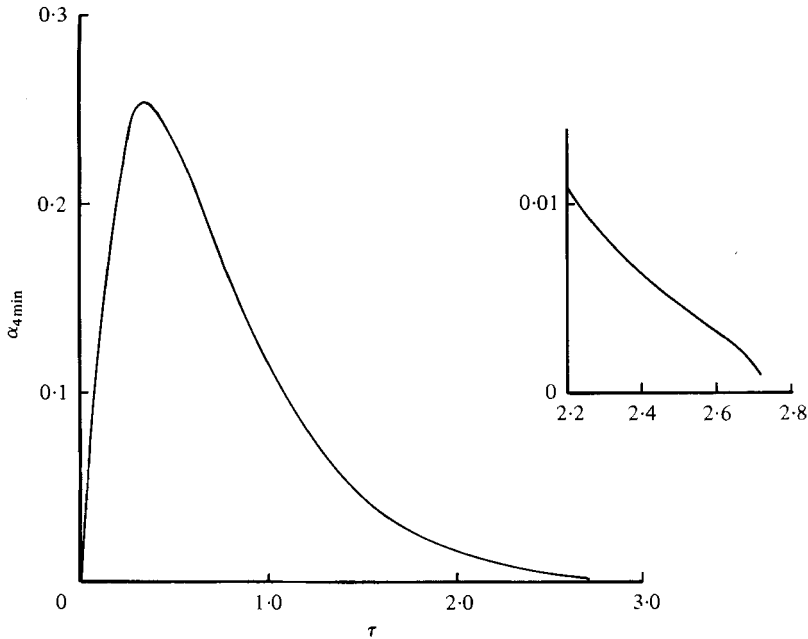


FIGURE 3. Variation of the minimum value of the coefficient  $\alpha_4$  with  $\tau$  ( $m = 0.2$ ).

the point where the boundary-layer thickness exceeds the value corresponding to  $\eta = 60$ , is shown in figure 2 as a dashed line. As expected, the value of  $f_w''$  for this case appears to asymptote the value  $-1.2326$  as predicted by Proudman & Johnson. It is interesting to note that for  $m = 0.8$ ,  $f_w''$  also appears to be approaching asymptotically the value  $-1.11136$  which is the inverse of the Falkner-Skan value for  $m = 0.8$ . Whether this particular result has any meaning, however, is open to question.

For values of the parameter  $m$  of 0.2, 0.4, or 0.6, the solutions were terminated fairly early, in terms of  $\tau$ , by a rapid increase in the number of iterations required to obtain convergence at each subsequent station until, at some station, convergence could not be obtained in a given large number of iterations. This is just the behaviour which is generally accepted to indicate the approaching of a singularity in the solution of the boundary-layer equations. This numerical behaviour, in itself, is not sufficient proof of a singularity. We therefore return to the equations of motion for an indication of the source of the numerical problems. The source of the difficulty is found when the momentum equation is written in the form shown in equations (17*a*, *b*). We note that if the coefficient  $\alpha_4$ , in equation (17*a*), vanishes at some point in the solution domain while the left-hand side of the equation does not vanish one can expect a singularity in the solution. To determine whether or not this is the case in the present calculations, the minimum value of  $\alpha_4$  at each station was calculated and its variation with  $\xi$  was tracked as the solution progressed. Figure 3 shows the variation of the minimum value of  $\alpha_4$ , at each station, with  $\tau$  for the case  $m = 0.2$ . Similar results were obtained for  $m = 0.4$  and  $m = 0.6$ . Figure 3 clearly shows that the numerical difficulties which lead to the termination of the solution are the result of the singularity associated with the vanishing, at a point in the flow field, of the coefficient  $\alpha_4$ .

In the physical plane, the singularity which terminates the flow for  $m = 0.2, 0.4$

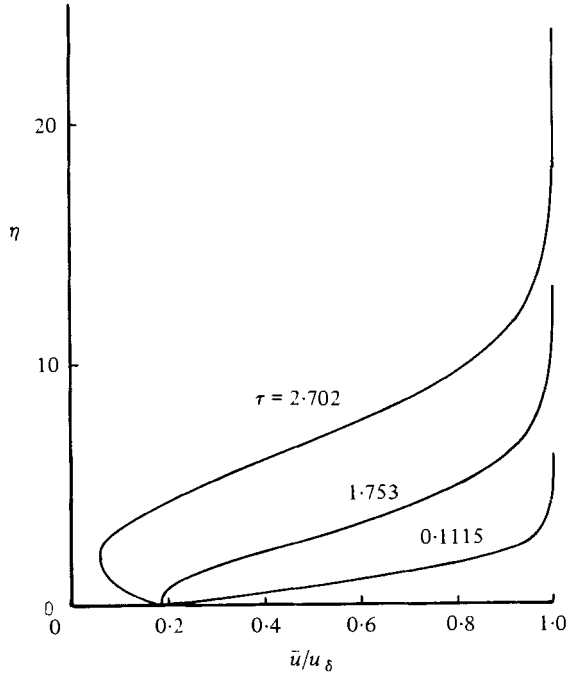


FIGURE 4. Velocity profiles, in a co-ordinate system moving with separation, at several values of  $\tau_1$  ( $m = 0.2$ ).

and 0.6 is a moving singularity. If we estimate, by extrapolation, that the singularity occurs at  $\xi_s$ , then from the second of equations (15) we have:

$$\xi_s = 1 - \exp[-cx_s^{m-1}t]$$

where  $x_s$  is the physical co-ordinate for the singular point. Hence,

$$x_s = \left( \frac{ct}{-\ln(1-\xi_s)} \right)^{1/(1-m)}$$

so that as the singular point moves away from the rear stagnation point (forward along the body) with increasing time. The speed at which the singular point moves is given by

$$U_s = \frac{dx_s}{dt} = \left( \frac{c}{-\ln(1-\xi_s)} \right)^{1/(1-m)} t^{m/(1-m)}.$$

It is instructive now to look at the velocity profiles at several values of  $\tau$  (or  $\xi$ ) as seen in a co-ordinate system which is moving with the singularity. Figure 4 shows velocity profiles at values of  $\tau$  of 0, 1.753, and 2.702 (values of  $\xi$  of 0, 0.97 and 0.9955, respectively) as seen in this moving co-ordinate system. Since  $\tau$  (or  $\xi$ ) is a combination of  $x$  and  $t$ , these three profiles may be viewed alternately as either the velocity profiles at three  $x$  stations as seen at a fixed time, or as velocity profiles at the same  $x$  station as seen at three different times. In the first case, increasing values of  $\xi$  correspond to decreasing values of  $x$ ; in the second case increasing values of  $\xi$  corresponding to increasing values of time. As  $\xi$  increases toward the value  $\xi_s$ , the velocity profile, in



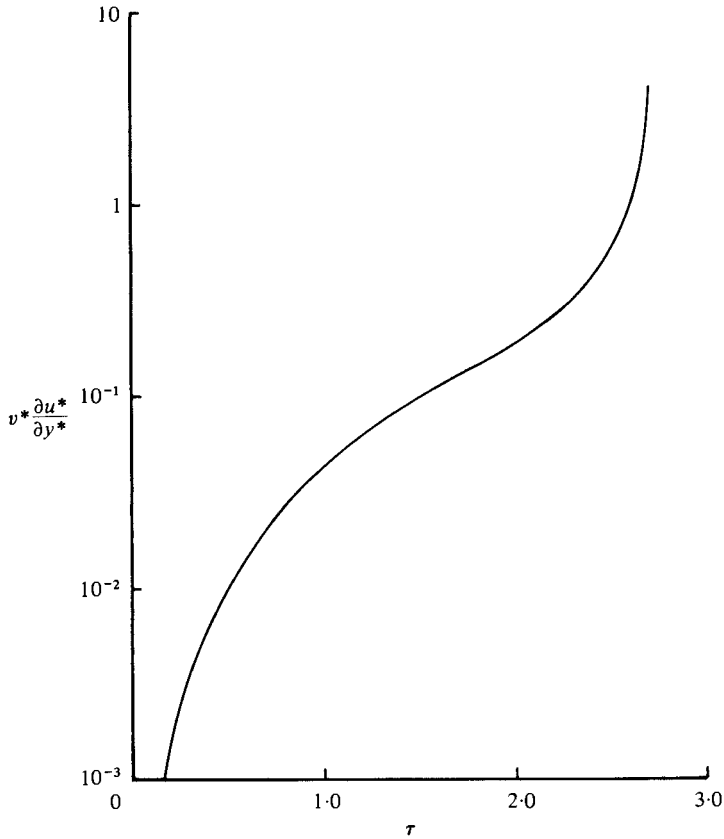


FIGURE 5. Vorticity transport normal to the wall,  $v^* \partial u^* / \partial y^*$ , at the point of maximum vorticity.

the moving co-ordinate system, approaches a profile in which both the shear and velocity approach zero simultaneously, at a point within the boundary layer. These are just the characteristics which have been proposed as corresponding to unsteady separation (the Moore–Rott–Sears model). Similar results are obtained for values of  $m$  of 0.4 and 0.6. The singularity which occurs in the solutions for moderate wedge angles is therefore clearly tied to separation of the unsteady boundary layer as predicted by the Moore–Rott–Sears model.

Finally, the non-dimensional time at which the wall shear vanishes,  $\tau_0$ , and the non-dimensional time at which separation occurs,  $\tau_s$ , are summarized in table 1 for the various values of  $m$ .

#### 4. Concluding remarks

A study has been made of the initial development, according to the boundary layer equations, of the flow in the vicinity of the sharp trailing edge of a symmetrical body which is impulsively set into motion. For the case where the trailing edge angle is  $\pi$ , there is a similar solution for the inviscid outer flow, as has been pointed out by Proudman & Johnson (1961). For all other trailing edge angles, however, no such inviscid solution exists.

---

$m$	$\tau_0$	$\tau_s$
0	—	—
0.2	1.675	2.772
0.4	0.819	1.750
0.6	0.541	1.555
0.8	0.404	—
1.0	0.322	—

---

TABLE 1. Non-dimensional times for zero wall shear,  $\tau_0$ , and for separation,  $\tau_s$ .

For a trailing edge with an included angle of zero ( $m = 0$ ) the solution is terminated to avoid large computational times and with the realization that the flow in the vicinity of the trailing edge will ultimately be influenced by the leading edge. For large trailing-edge angles, the solutions are terminated due to excessive boundary-layer thicknesses. For moderate trailing edge angles, the solutions are terminated by the approaching of a singularity in the solutions to the boundary-layer equations. In the physical plane this singularity moves up the body from the trailing edge. It is shown that in a co-ordinate system moving with the singularity, as the flow approaches the singularity the velocity profile approaches one in which the shear and velocity vanish simultaneously at some point within the boundary layer. These results thus substantiate the Moore–Rott–Sears model for unsteady separation, at least in the case where the separation point moves forward along the body.

In recent years a number of investigators have presented solutions to the boundary-layer equations which substantiate the Moore–Rott–Sears model for unsteady boundary layer separation. Until recently, however, there has been no adequate description of the physical process of separation – no description that would tie both steady and unsteady separation together. Recently, van Dommelen & Shen (1981) have provided a clear and unambiguous description of flow separation. They indicate that separation, either steady or unsteady, is defined as the ‘point where a vorticity streak departs from the wall’. They speak further of the ‘ejected vorticity layer’. This process of separation can be seen in the present results. A strong layer of vorticity forms immediately adjacent to the wall early in the flow. At the time when the local velocity profile has an inflection, this layer of vorticity moves off the wall but remains close to it. Even after the point of zero shear passes a local station, the vorticity layer remains relatively close to the wall. Within the limits of boundary-layer theory, the vorticity  $\omega$  is given by  $\omega = -\partial u/\partial y$ . The presence of the layer of vorticity at various positions relative to the wall is shown in figure 4. The layer of strong vorticity is clear in these velocity profiles. We note the second vorticity layer being generated on the wall by the reverse flow beyond the point of zero wall shear.

The concept of separation involves more than just the location of the vorticity layer. It involves also the idea of ejection of the vorticity layer. That such ‘ejection’ occurs and is indeed associated with the singularity is shown in figure 5 where the product of the maximum shear  $\partial u^*/\partial y^*$  and the corresponding vertical velocity  $v^*$  is plotted as a function of  $\tau$ , again for  $m = 0.2$ . Similar results are obtained for  $m = 0.4$  and  $0.6$ .

For small  $\tau$  the shear layer lies on the wall (figure 4) and the vertical velocity is small so that the rate at which vorticity is transported normal to the wall is small (figure 5). Beyond  $\tau \simeq 0.105$  (the point at which there is an inflection point in the

velocity profile), the peak in vorticity rises off the wall (figure 4) but the vertical velocities are small and so the vorticity transport normal to the wall remains small. Beyond  $\tau \simeq 1.642$  (the point of zero wall shear), the peak in the vorticity rises further off the wall (figure 4) and, while the vertical component of velocity is increasing, it is still relatively small and so the net vorticity transport normal to the wall is still relatively small. Only as  $\tau$  approaches the singularity ( $\tau \simeq 2.702$ ) does the point of maximum vorticity move quite far from the wall while the normal component of velocity becomes quite large so that the normal transport of vorticity increases rapidly. Thus we now have a complete description of the physical phenomenon of separation. A layer of strong vorticity is initially generated at the wall, then slowly moves off the wall and finally is ejected from the vicinity of the wall by the strong vertical velocity associated with separation. It is important to note that this description of separation applies equally well to both steady and unsteady flows.

## REFERENCES

- BLOTTNER, F. G. 1970 Finite-difference methods of solution of the boundary layer equations. *A.I.A.A. J.* **8**, 193.
- DENNIS, S. C. R. 1972 The motions of a viscous fluid past an impulsively started semi-infinite flat plate. *J. Inst. Math. Applic.* **10**, 105.
- HALL, M. G. 1969 The boundary layer over an impulsively started plate. *Proc. R. Soc. Lond. A* **310**, 401.
- NANBU, K. 1971 Unsteady Falkner-Skan flow. *Z. angew. Math. Phys.* **22**, 1167.
- PROUDMAN, I. & JOHNSON, K. 1961 Boundary layer growth near a rear stagnation point. *J. Fluid Mech.* **12**, 161.
- ROBINS, A. J. & HOWARTH, J. A. 1972 Boundary layer development at a two-dimensional rear stagnation point. *J. Fluid Mech.* **56**, 161.
- SMITH, S. H. 1967 The impulsive motion of a wedge in a viscous fluid. *Z. angew. Math. Phys.* **18**, 508.
- STEWARTSON, K. 1951 On the impulsive motion of a flat plate in a viscous fluid. *Quart. J. Mech. Appl. Math.* **4**, 182.
- VAN DOMMELEN, L. L. & SHEN, S. F. 1981 The genesis of separation. In *Numerical and Physical Aspects of Aerodynamic Flows, Proc. Symp. January 1981, Long Beach, California* (ed. T. Cebeci).
- WILLIAMS, J. C. & JOHNSON, W. D. 1974 Semisimilar solutions to unsteady boundary layer flows including separation. *A.I.A.A. J.* **12**, 1388.
- WILLIAMS, J. C. & RHYNE, T. B. 1980 Boundary layer development on a wedge impulsively set into motion. *SIAM J. Appl. Math.* **38**, 215.